Disruption Mitigation in the Presence of Pre-existing MHD Instabilities

D. Shiraki[1], R.A. Granetz[2], N. Commaux[1], L.R. Baylor[1], D. Brunner[2], C.M. Cooper[3], N.W. Eidietis[4], E.M. Hollmann[5], A. Kuang[2], C.J. Lasnier[6], R.A. Moyer[5], C. Paz-Soldan[4], R. Raman[7], M.L. Reinke[1], A. Tinguely[2]

[1]Oak Ridge National Laboratory, Oak Ridge, TN 37831, USA
[2]Massachusetts Institute of Technology, Cambridge, MA 02139, USA
[3]Oak Ridge Associated Universities, Oak Ridge, TN 37831, USA
[4]General Atomics, San Diego, CA 92186, USA
[5]University of California-San Diego, La Jolla, CA 92093, USA
[6]Lawrence Livermore National Laboratory, Livermore, CA 94551, USA
[7]University of Washington, Seattle, WA 98195, USA

E-mail contact of main author: shirakid@fusion.gat.com

Abstract. Experiments on the DIII-D and Alcator C-Mod tokamaks show that disruption mitigation techniques by massive high-Z impurity injection remain effective in the presence of large pre-existing magnetohydrodynamic (MHD) instabilities. Rotating and locked magnetic islands will precede a large fraction of disruptions in ITER, making their impact on disruption mitigation a critical concern. Experiments on the two machines have compared the effectiveness of mitigation techniques with and without pre-existing MHD instabilities prior to injection, showing that such modes do not significantly impede the ability of massive impurity injection to mitigate thermal quench (TQ) and current quench (CQ) loads. The existence of locked modes preceding the impurity injection results in faster plasma cooling durations, but no significant degradation of the radiated fraction or heat load mitigation is observed. TQ particle assimilation increases after the onset of minor disruptions, implying an increase in the MHD mixing of injected impurities in these cases. CQ metrics are found to be very reproducible in all injection scenarios, consistent with CQ plasma evolution being fairly symmetric and thus independent of the effects of MHD activity preceding the TQ. Both of ITER's disruption mitigation technologies, shattered pellet injection and massive gas injection, are shown to remain effective in these studies. These results demonstrate the applicability of previous disruption mitigation studies which typically did not have large MHD activity prior to injection, providing further confidence in the established physics basis for disruption mitigation in ITER.

1. Introduction

Major disruptions pose a significant challenge for ITER, where unmitigated thermal quench (TQ) heat loads and current quench (CQ) electromagnetic forces have the potential to cause significant damage to the device [1]. Thus it will be critical to mitigate such disruption loads through rapid shutdown by massive high-Z impurity injection, which reduces peak TQ heat loads through radiative dissipation of the thermal energy, and decreases CQ halo current forces by increasing the plasma resistivity and resulting plasma current decay rate [2]. The ITER disruption mitigation system (DMS) will implement this massive impurity injection based on two methods: shattered pellet injection (SPI) and massive gas injection (MGI) [3]. The SPI technique injects the required impurities as a solid cryogenic pellet which is shattered just prior to entering the plasma [4,5], while MGI injects the particles as a high pressure gas pulse [6].

While these disruption mitigation techniques have been demonstrated in present-day tokamaks, many of these experiments have studied only the rapid shutdown of high-performance H-mode discharges, which typically do not suffer from large magnetohydrodynamic (MHD) instabilities. This is advantageous for providing a controlled

repeatable target discharge, as well as for demonstrating the radiative dissipation of high thermal energies (as will be required in future large devices). However, a large number of disruptions in ITER are expected to be preceded by large rotating or locked magnetic islands, based on experience from present-day devices [7,8]. Thus the impact of such pre-existing MHD instabilities on the effectiveness of disruption mitigation techniques is a critical concern. Some present-day devices routinely trigger the DMS based on real-time information including MHD signals [9,10], though such routine use across a variety of scenarios does not necessarily allow a controlled study of the influence of the MHD modes on the mitigation process. Experiments on ASDEX Upgrade have compared MGI in plasmas with and without locked modes, showing that the presence of such modes can reduce the particle assimilation prior to the TQ (primarily by reducing the time between the initial particle delivery and the TQ onset) [11].

In this paper, we describe results from similar controlled experiments on DIII-D and Alcator C-Mod, which compare the effectiveness of disruption mitigation techniques with and without large pre-existing MHD instabilities. Both of the ITER DMS technologies, SPI and MGI, were included in these studies, and the results of these experiments suggest that the effectiveness of these techniques is not significantly impeded by the presence of such MHD modes. These results, which improve confidence in the applicability of previous disruption mitigation works, are presented as follows. Section 2 describes the setup of the experiments carried out on each device. Sections 3 and 4 describe 0D global properties of the TQ and CQ, respectively. Section 5 describes potential toroidal asymmetries during the mitigated disruption. Section 6 is a summary of results.

2. Experimental Setup

Experiments on DIII-D and Alcator C-Mod have each investigated the impact of pre-existing MHD activity on disruption mitigation techniques. Here we describe the experimental scenarios used on each device.

2.1. DIII-D

The target plasmas in these experiments were ITER baseline scenario discharges, with safety factor (at the 95% flux surface) $q_{95} = 3.1$ and normalized plasma beta $\beta_N = 1.8$. Plasma currents were 1.3 MA, with a toroidal field of 1.7 T. At low injected torques, these plasmas generate $m/n = 3/2$ or $2/1$ (or both) tearing modes (where m/n are the poloidal/toroidal mode numbers), which subsequently lock to the wall (typically within 200 ms), resulting in a 2/1 locked mode. Besides correction of the intrinsic error field, no external magnetic perturbations are applied. These discharges are initially in H-mode, but transition back to L-mode when the plasma locks. The plasmas have 4 MW of neutral beam heating, resulting in a stored energy of 0.75 MJ during H-mode, which decreases to ~0.25 MJ after locking (over several hundred milliseconds). Both MGI and SPI were tested in these experiments, with injections from a low-field side upper port location. Pure neon was used for both mitigation methods, with injection quantities of 27 Pa-m^3 for MGI, and 53 Pa-m^3 for SPI. The SPI/MGI were triggered at various times relative to the MHD growth:

1. During the H-mode portion of the discharge (prior to tearing mode onset).

2. During the rotating tearing mode phase (prior to locking). The plasmas still have H-mode confinement in this phase.

3. After the plasma locks, with varying time delay after locking (but prior to an unmitigated disruption).

In the absence of SPI/MGI, an unmitigated disruption occurs within ~500 ms of the plasma locking. These unmitigated cases are also compared.

2.2. Alcator C-Mod

In the Alcator C-Mod experiments, the target plasmas were L-mode discharges, with plasma currents of 1 MA and a toroidal field of 5.4 T. The MHD modes in these discharges were *m/n* = 2/1 locked modes, resulting from the penetration of externally applied *n* = 1 error fields. These discharges had 1 MW of ion cyclotron heating, resulting in a stored thermal energy of 0.05 MJ, with magnetic stored energies of 0.75 MJ. MGI was used for mitigation, with injections from the low-field side slightly below the midplane at two toroidal locations. Injection quantities were 250 Pa-m^3, with mixtures of 15% argon and 85% helium (which has been shown in previous studies to balance fast time response with effective mitigation [12]). MGI in plasmas with and without the locked modes were compared, along with unmitigated cases which disrupt due to a small impurity puff (with quantities which are too small for mitigation).

3. Thermal Quench Properties

The goal of the DMS for thermal mitigation is to inject a large quantity of high-*Z* impurities prior to the end of the TQ, in order to increase the radiation fraction and thereby reduce the conducted heat loads to the divertor. Thus, the particle assimilation, radiation fraction, and resulting divertor heating are key metrics for the efficiency of TQ mitigation.

The TQ particle assimilation in the plasma is partly constrained by the plasma cooling duration, defined here to be the time between the arrival of the initial particles at the plasma edge and the end of the TQ (when the CQ begins). This parameter, which is only defined in cases with impurity injections, is an important quantity, as it is the time during which impurities entering the plasma can still contribute to TQ heat load mitigation. Figure 1 shows that this cooling timescale following MGI in DIII-D is shortened by ~25% when injecting into plasmas with locked modes, compared to injections in H-mode plasmas (including those with rotating tearing modes). Because these plasmas transition back to L-mode after locking, it is unclear whether this change occurs simply through equilibrium effects or as the result of non-axisymmetric

Fig. *1. (DIII-D) Plasma cooling durations following MGI are shorter in plasmas with locked modes. The locked mode cases are shown as a function of the timing delay between locking and MGI.*

MHD effects. Measured cooling durations for SPI into locked plasmas are comparable to those for MHD-free L-mode plasmas, although the limited number of cases (only two discharges) makes the comparison difficult. However, this associated confinement drop follows as a consequence of the plasma locking, so that the resulting shortening of the cooling duration can be expected to be a ubiquitous result, independent of the mechanism responsible. A similar reduction of the timescales leading to the TQ were reported for low-field side MGI on ASDEX Upgrade [11]. However, despite this shortened timescale available for the
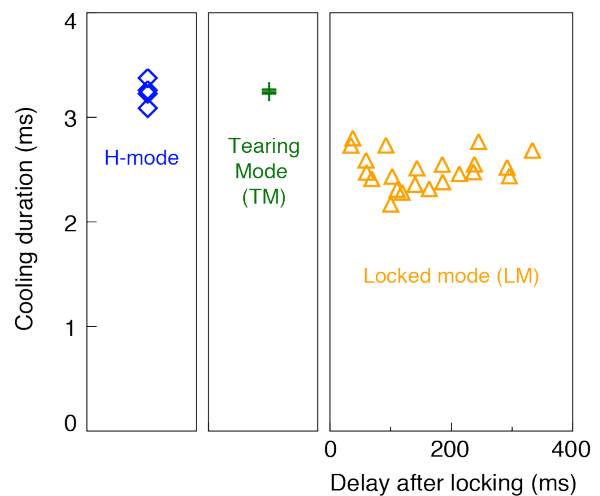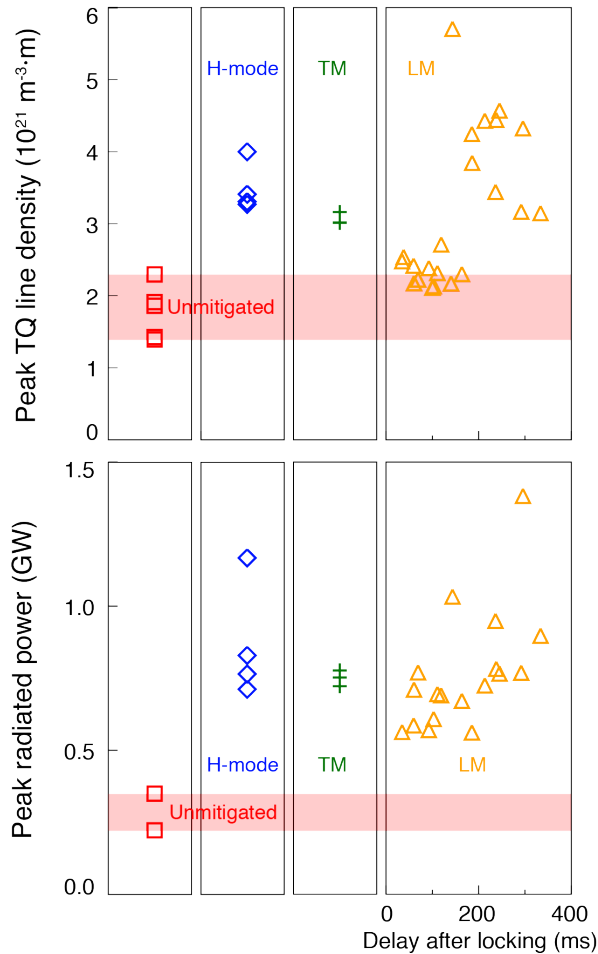
Fig. 2. (DIII-D) Peak TQ densities in locked mode plasmas are reduced for earlier MGI, but enhanced for later injections. Radiated powers follow a similar trend, but are significantly higher than unmitigated disruptions for all cases.

injection of radiating impurities, radiation fractions and protection of the divertor are not negatively impacted, as will be shown.

Figure 2(a) shows that for MGI within ~200 ms of the plasma locking, peak TQ densities are reduced relative to H-mode plasmas. This is potentially attributable to the reduced cooling duration shown in Figure 1, as is the interpretation for reduced fueling during high-field side MGI in locked ASDEX Upgrade plasmas [11]. However, for later injections, the particle assimilation actually increases, including cases which exceed the H-mode discharges. This increased assimilation may be due to enhanced MHD mixing as the plasma stability is degraded, as evidenced by the onset of minor disruptions after ~200 ms (and major disruption occurring within ~500 ms if no impurity injection takes place). These observations in DIII-D differ from the ASDEX Upgrade results, where locked modes had little effect on the particle assimilation from low-field side MGI [11], but this difference is not yet understood. It should be noted that the densities shown here are the highest values measured *during the TQ*, but densities continue to rise beyond this, reaching peak values during the CQ, as described in Section 4. For the Alcator C-Mod discharges, peak density data are not available due to refraction of the interferometer at high densities.

However, despite possible reductions in particle assimilation for the early MGI cases in locked plasmas, the peak radiated power in all cases are found to be significantly higher with MGI than without, independent of the MHD activity, as shown in Figure 2(b). This is believed to be due to the highly radiative nature of the injected neon or argon, which radiate efficiently even with relatively low quantities [12,13]. In Alcator C-Mod, radiation fractions measured over the entire disruption are likewise unaffected by the locked mode, with no significant difference observed between locked and unlocked mitigated disruptions. In the DIII-D data (Figure 2(b)), peak radiated powers in the locked cases are found to increase along with the MGI delay, consistent with the trend in the density. (However in addition, radiation asymmetries may also contribute to this trend, as is discussed in Section 5.) Similar results are found for SPI (not shown), where radiated powers are significantly elevated relative to unmitigated disruptions, with or without the locked modes. However, the small number of cases available makes it difficult to determine any trends with the MGI timing.

Of course, the most important metric for TQ mitigation is the divertor heat loads, which must be mitigated in order to minimize melting and erosion. The resulting post-disruption surface temperatures in the divertor and first wall of DIII-D are calculated from infrared imaging. Figure 3 shows the temperature at the inner strike point, due to the heat loads from

unmitigated and SPI mitigated disruptions. Consistent with the measured increases in TQ radiation fractions, divertor heating is effectively reduced from unmitigated values, for all cases with SPI (with or without tearing modes and locked modes). Similar reductions are observed for MGI mitigation.

Thus overall, the existence of large pre-existing MHD instabilities prior to injection is not found to impede TQ mitigation by MGI or SPI. Although the plasma cooling duration is shortened in plasmas with locked modes, mitigation of the divertor heat loads by the massive impurity injection is comparable with or without the MHD modes.

Fig. 3. (DIII-D) SPI reduces heat loads at the inner strike point, relative to unmitigated values.

4. Current Quench Properties

Due to its low-Z beryllium first wall, ITER is expected to have long CQ timescales and large halo currents in the absence of mitigation, and the DMS will be required to accelerate this current decay rate [1]. In addition, the DMS aims to raise the peak electron density during the CQ, in order to increase the collisional dissipation of seed runaway electrons [14].

Measured CQ durations from both machines are shown in Figure 4, for unmitigated and MGI mitigated disruptions. For both Alcator C-Mod and DIII-D, MGI is found to be equally effective in accelerating the CQ with or without the MHD activity, with very reproducible CQ rates. In DIII-D, the measured CQ duration is found to be essentially independent of the timing of the MGI relative to the locking. The same level of reproducibility is observed for mitigation by SPI. These results indicate that 3D MHD effects have very little impact on the global evolution of the CQ plasma, which is consistent with expectations from previous analyses of mitigated disruptions indicating that the CQ dynamics are typically uniform and symmetric [6,15]. Peak-to-peak values of the vacuum vessel displacement due to CQ halo
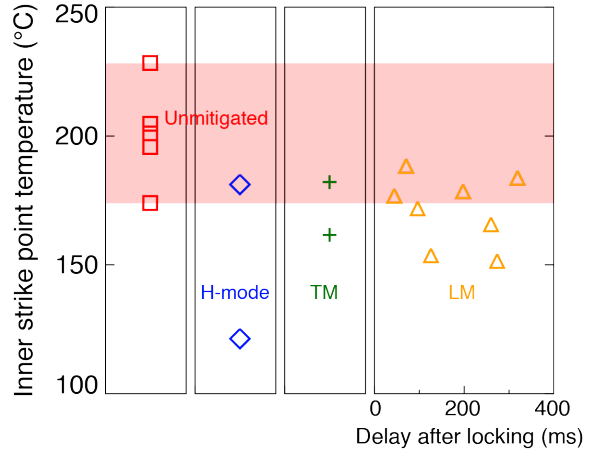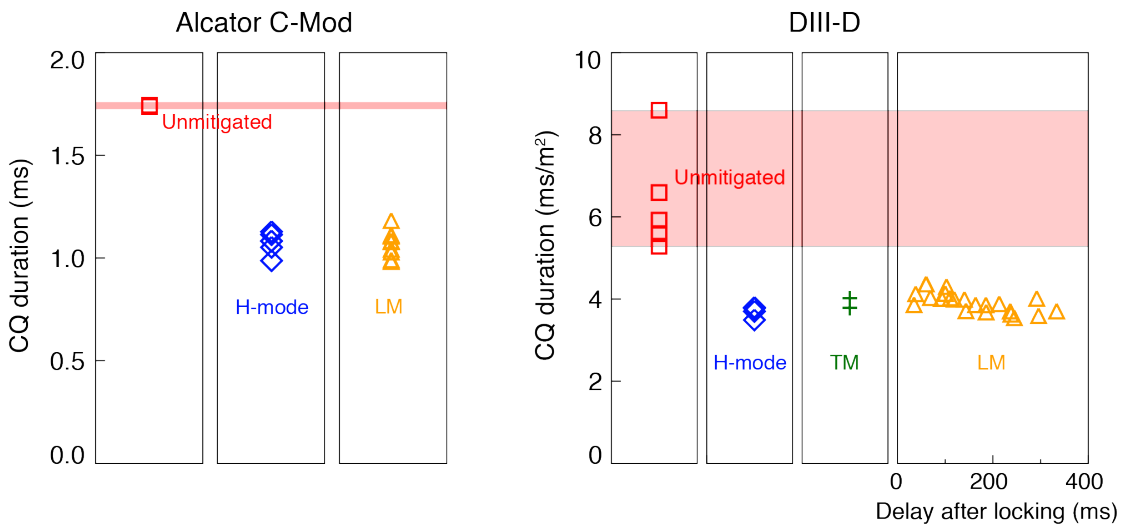

Fig. 4. (C-Mod, DIII-D) MGI reproducibly reduces CQ timescales, with or without pre-existing MHD modes, in both Alcator C-Mod and DIII-D. Locked plasma cases in DIII-D are shown as a function of the delay between locking and MGI.
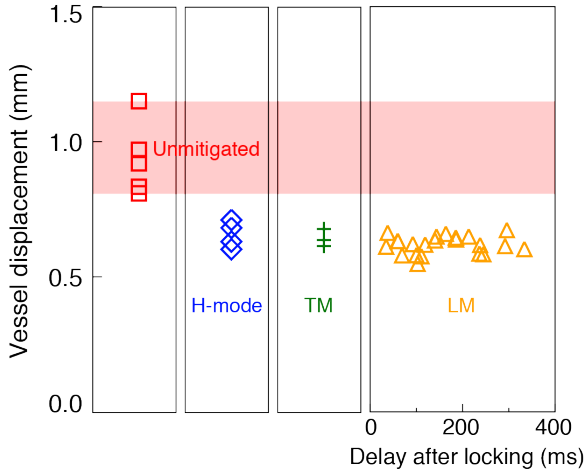
Fig. 5. (DIII-D) Vacuum vessel displacement is effectively mitigated in all cases with MGI.
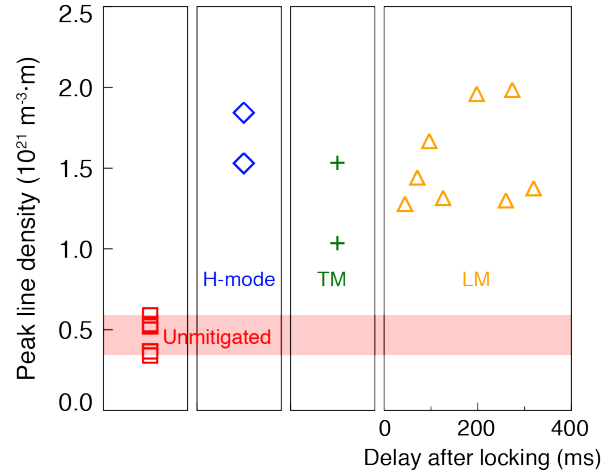

Fig. 6. (DIII-D) Peak line-integrated densities during the CQ, for unmitigated and SPI mitigated disruptions.

current forces, are shown in Figure 5 for MGI in DIII-D. The mitigation of this vessel motion exhibits the same trend as the CQ timescales, with effective reduction in amplitude and scatter observed in all cases with MGI, with or without pre-existing MHD modes. Mitigation of the vessel displacement by SPI is similar to that shown in Figure 5.

For runaway electron suppression, SPI has demonstrated the highest CQ densities to date on DIII-D, and is believed to have the higher likelihood of the two ITER DMS technologies for achieving full suppression of runaway growth [16]. The peak electron densities (over the entire disruption) achieved by SPI, which occur early in the CQ [5], are shown in Figure 6. Although injection quantities here are scaled for TQ mitigation and not for runaway electron dissipation, the electron densities following SPI are significantly elevated from the unmitigated cases, with no significant differences observed between the discharge types.

Thus, these results from DIII-D and Alcator C-Mod show that the ability of high-Z MGI and SPI to accelerate the CQ rate, mitigate halo current forces, and raise the CQ electron density, is unimpeded by the existence of MHD modes prior to injection. The low scatter in observed CQ plasma evolution characteristics suggests that the CQ dynamics are determined more strongly by injection properties and are relatively insensitive to 3D MHD effects.

5. Toroidal Asymmetries

Previous works have shown that radiation asymmetries in a rapid shutdown can be driven by the $n = 1$ MHD growth during the TQ, with the location of the peak determined by the toroidal phase of the island [15,17]. Because the MHD heat flux is a major driver of such asymmetries [18], possible enhancement of such asymmetries is a concern in the presence of large pre-injection modes.

On Alcator C-Mod, a toroidal array of five photodiodes allows the toroidal peaking of the radiated power to be quantified in a single shot [19]. Examples of this measured toroidal peaking factor (TPF) for locked and unlocked cases are shown in Figure 7. These measurements do not show significant differences in radiation asymmetries between the two cases. Asymmetries are particularly of concern during the large TQ radiation flash, but the measured TPFs are comparable for both cases, and remain below 2 (which is the estimated limit for ITER [20]).

In DIII-D, radiation measurements are only available at one toroidal location. Thus, while the measured radiated powers in Section 3 were interpreted as global quantities, asymmetries may impact these results. Indeed, calculated radiation fractions (assuming toroidal symmetry) exceed 100% in many of the locked cases with late MGI, implying that some level of peaking likely does exist. However, because no efforts were made to control the locked mode toroidal phase (which is instead determined by the influence of viscous torques from the plasma, neutral beams, etc.), the resulting phases are found to fall within a rather narrow range of ~90°. A systematic change in island phase with time (relative to locking) is observed,
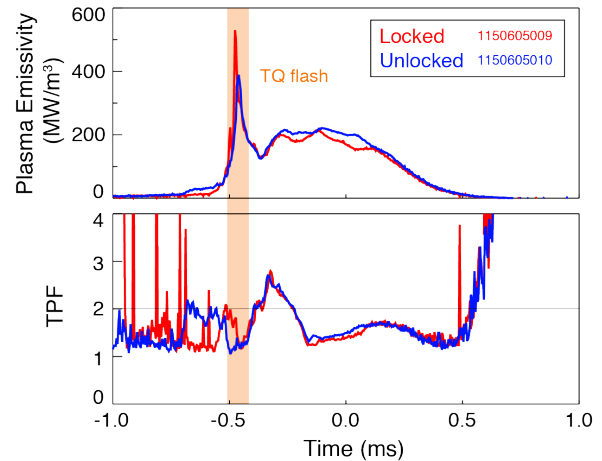

Fig. 7. (C-Mod) Toroidal peaking factors (TPF) during the TQ radiation flash are comparable for MGI in locked and unlocked plasmas.

which is consistent with the increase in radiation shown in Figure 2(b) being at least partially due to toroidal asymmetries. However, due to the limited range of mode phases, the degree of peaking cannot be determined from these data as has been done in [15].

Thus, Alcator C-Mod results suggest that toroidal radiation peaking is not significantly enhanced by the existence of a locked mode, while the DIII-D results are inconclusive. However, the locking of a high-performance plasma is typically accompanied by a large drop in the stored energy, making radiation asymmetries a less critical concern. Similar conclusions are reached in ASDEX Upgrade, where locked modes are reported to contribute to large asymmetries during the pre-TQ phase, but only in cases where thermal energies are reduced to levels which would not be expected to cause melting of the ITER wall [11].

6. Summary

Experiments on the DIII-D and Alcator C-Mod tokamaks show that the effectiveness of the SPI and MGI techniques for disruption mitigation are largely unimpeded by the presence of large pre-existing MHD instabilities prior to injection. The plasma cooling duration is reduced in the presence of locked modes, but the highly radiative impurities assimilated in this timescale remain effective in dissipating the plasma thermal energy and mitigating divertor heat loads. In cases with MGI occurring well after locking, TQ particle assimilation actually increases, likely due to enhanced MHD mixing. Acceleration of the CQ rate and reduction of halo current forces are reliably achieved by either injection method, and the low scatter observed in CQ metrics suggest that CQ dynamics are fairly symmetric and independent of MHD effects. Pre-disruption MHD instabilities also do not significantly impact the peak CQ densities achieved by SPI. No evidence is seen of toroidal asymmetries which exceed those occurring during rapid shutdown of a MHD stable discharge. These results demonstrate the applicability of previous disruption mitigation studies without large MHD instabilities, and improve confidence in the existing physics basis for disruption mitigation by SPI and MGI.

7. Acknowledgement

References

[1] LEHNEN, M., et al., J. Nucl. Mater. **463** (2007) S128

[2] HENDER, T.C., et al., Nucl. Fusion **47** (2007) S128

[3] BAYLOR, L.R., et al., Fusion Sci. Tech. **68** (2015) 211

[4] COMBS, S.K., et al., IEEE Transactions on Plasma Science **38** (2010) 400

[5] COMMAUX, N., et al., Nucl. Fusion **56** (2016) 046007

[6] HOLLMANN, E.M., et al., Nucl. Fusion **48** (2008) 115007

[7] DE VRIES, P.C., et al., Phys. Plasmas **21** (2014) 056101

[8] PAUTASSO, G. et al., Proceedings of the 41st EPS Conference on Plasma Physics, Berlin, Germany (2014) P2.015

[9] REUX, C., et al., Fusion Eng. Des. **88** (2013) 1101

[10] PAUTASSO, G., et al., Nucl. Fusion **47** (2007) 900

[11] PAUTASSO, G., et al., Proceedings of the 40th EPS Conference on Plasma Physics, Helsinki, Finland (2013) O5.104

[12] BAKHTIARI, M., et al., Nucl. Fusion **51** (2011) 063007

[13] SHIRAKI, D., et al., Phys. Plasmas **23** (2016) 062516

[14] ROSENBLUTH, M.N., PUTVINSKI, S.V., Nucl. Fusion **37** (1997) 1355

[15] SHIRAKI, D., et al., Nucl. Fusion **55** (2015) 073029

[16] COMMAUX, N., et al., Nucl. Fusion **50** (2010) 112001

[17] LEHNEN, M., et al., Nucl. Fusion **55** (2015) 123027

[18] IZZO, V.A., Phys. Plasmas **20** (2013) 056107

[19] OLYNYK, G.M., et al., Nucl. Fusion **53** (2013) 092001

[20] SUGIHARA, M., et al., Nucl. Fusion **47** (2007) 337